Supporting Information

Supplemental Figure 1: NAD^+ saturation curves with SIRT1, SIRT2, SIRT3, and SIRT6 and various acylated peptides. Assays were performed at saturating acetyl-, hexanoyl-, decanoyl-, and myristoyl-lysine H3K9 peptide concentrations. Time points were selected so that steady-state initial velocities were maintained in all reactions. ($n \geq 3$, ± standard deviation)

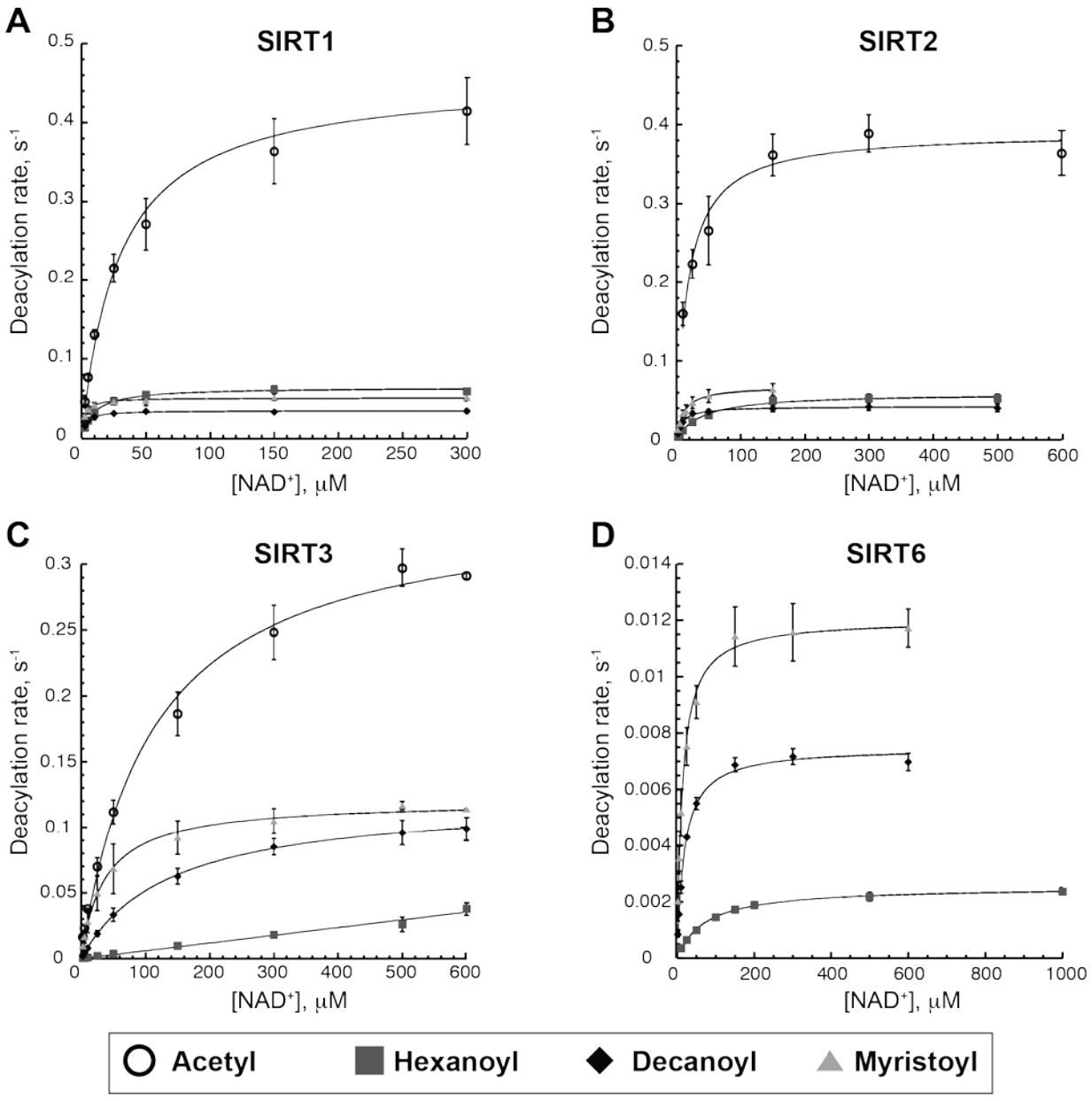

Supplemental Figure 2: Effect of nicotinamide inhibition on the deacylases activity of SIRT1, SIRT2, SIRT3 and SIRT6. Assays were performed at saturating concentrations of acetyl-, hexanoyl-, decanoyl-, and myristoyl-lysine H3K9 peptides and NAD^+. Time points were selected so that steady-state initial velocities were maintained in all reactions. ($n \geq 2$, ± standard deviation)

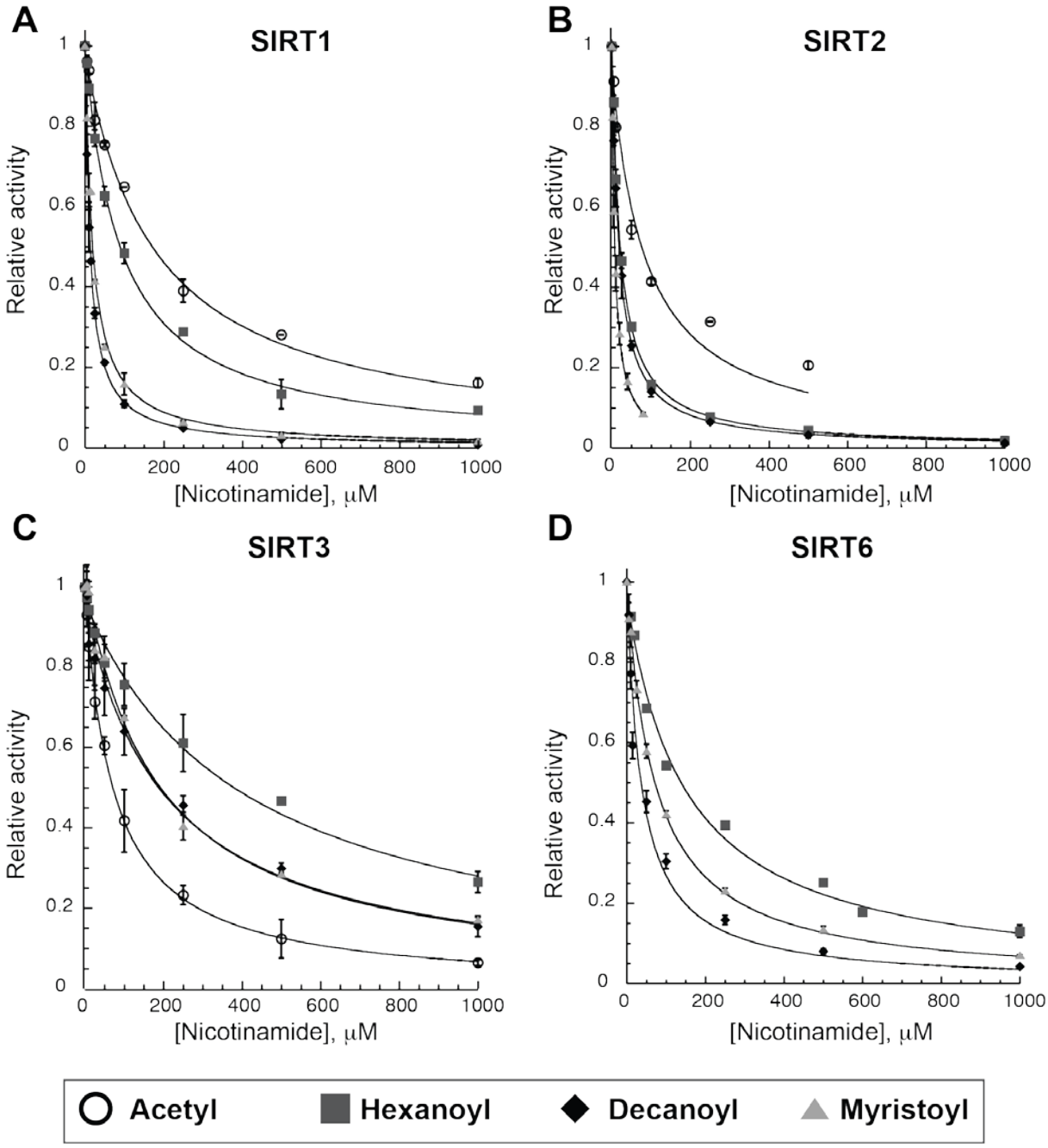

Supplemental Figure 3: Single turnover kinetic analysis of SIRT2, SIRT3, and SIRT6. Single turnover kinetic analysis of SIRT2, SIRT3, and SIRT6 monitoring nicotinamide formation and deacylated peptide formation. *A*, SIRT2 (12 μM) was incubated with 2.5 μM acetyl-, hexanoyl-, decanoyl-, and myristoyl-peptide in the presence of 400 μM NAD^+. *B*, SIRT3 (12 μM) was incubated with 2.5 μM acetyl-, hexanoyl-, decanoyl-, and myristoyl-peptide in the presence 600 μM NAD^+ or 2 mM NAD^+ with hexanoylated peptide. *C*, SIRT6 (18 μM) was incubated with 5 μM hexanoyl-, decanoyl-, and myristoyl-peptide in the presence of 300 μM NAD^+.

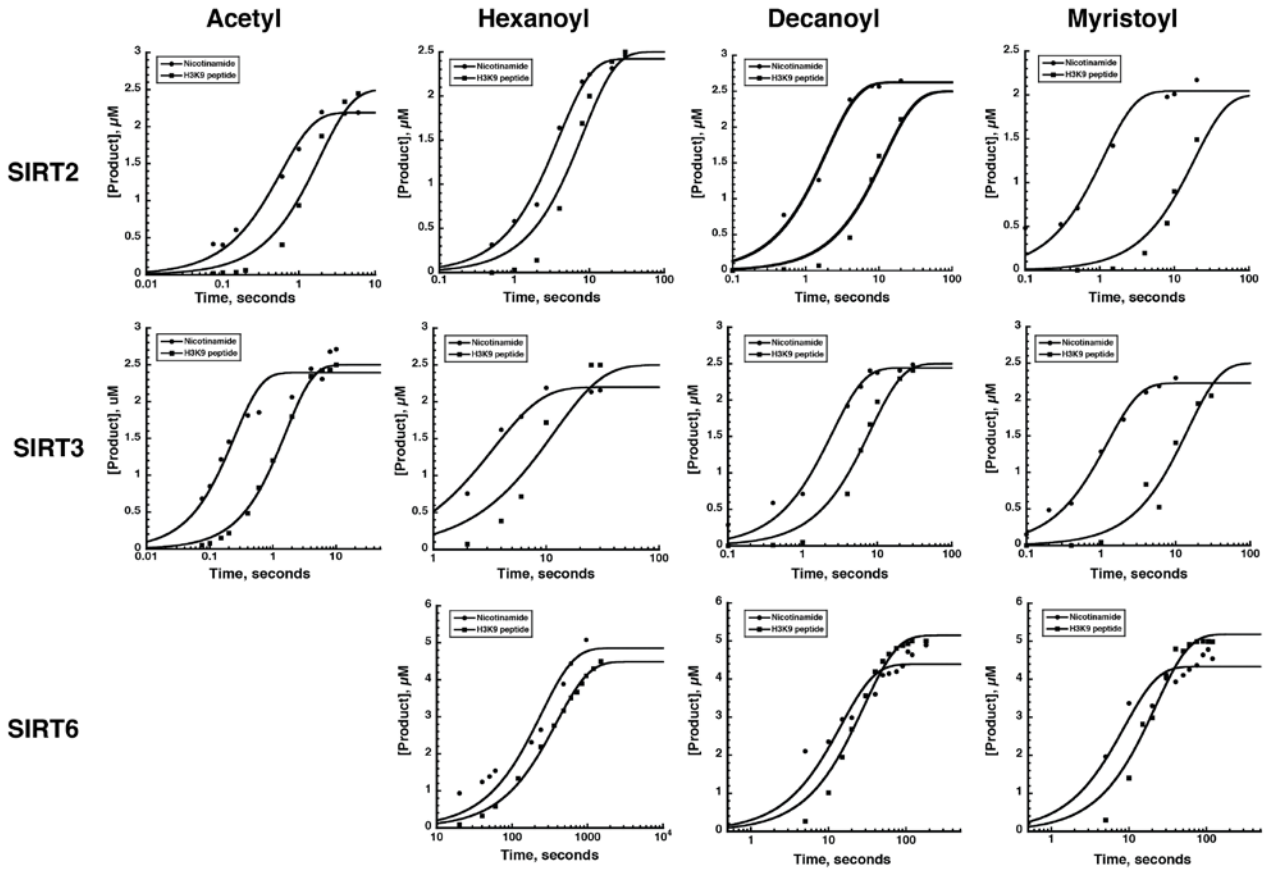

Supplemental Figure 4: Re-refinement of myristoyl-lysine residue in crystal structure of SIRT6 in complex with TNF-αK20myr peptide (PDB ID: 3ZG6). 2Fo-Fc omit electron density map (grey mesh, 1σ) of the myristoylated Lysine and water molecule (A2146). *A*, Substrate peptide, the water molecule and the active site His 131 of SIRT6 in PDB ID: 3ZG6 are drawn. Orange dotted lines show the close contact between the myristoylated lysine residue and the water molecule. The distances from the water molecule to Nζ and Cε of the residue are 2.0 and 2.2 Å, respectively. The water molecule is 3.7 Å away from the active site His 131 (yellow dotted line is drawn for reference). *B*, Re-refined structure of myristoylated lysine in a trans conformation is drawn.

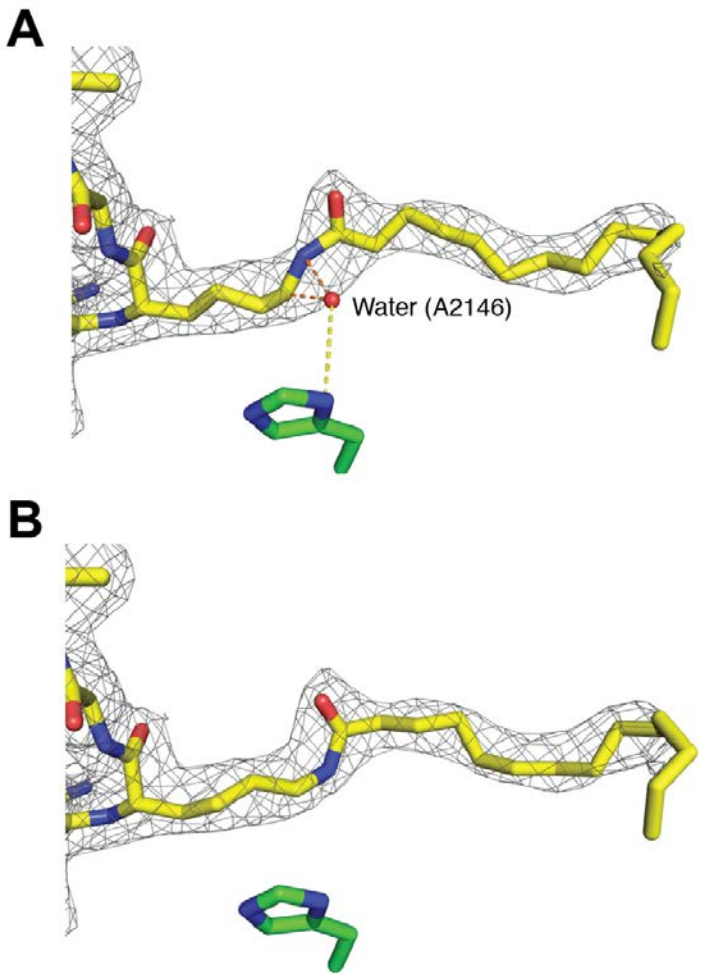

Supplemental Figure 5: Sequence alignment of human Sirtuins SIRT1 – SIRT5. The amino acid sequences of the catalytic domains of human SIRT1 – SIRT5 were aligned using the online version of ClustalW. The conserved helix bundle region is enclosed in a black box. The amino acids located in α-helix 4 and α-helix 6 of SIRT2 that show the greatest movement in the presence of the myristoyl chain are boxed in red. The additional amino acids in the hydrophobic cavity of SIRT2 are boxed in blue. SIRT6 and SIRT7 do not contain a helix bundle region and were excluded.

Supplemental Table 1: Rate constant comparisons.

SIRT2 and SIRT3 $k_{cat}/K_{m,\ NAD}$, k_5, k_{cat} and k_9 rates as well as K_m were analyzed relative to the acetylated substrate (acetyl/acyl) to determine the effect of acyl chain on the rate. SIRT6 $k_{cat}/K_{m,\ NAD}$, k_5, k_{cat} and k_9 rates as well as K_m were analyzed relative to the myristoylated substrate (myristoyl/acyl). SIRT1 $k_{cat}/K_{m,\ NAD}$, k_{cat} and K_m were analyzed relative to the acetylated substrate.

SIRT2 – Relative decrease compared to Acetyl (acetyl/acyl)

	k_{cat}/K_m	k_5	k_{cat}	k_9	K_m
Acetyl	1.0	1.0	1.0	1.0	1.0
Hexanoyl	14.7	5.5	6.6	4.8	0.5
Decanoyl	4.5	3.7	9.3	5.9	2.1
Myristoyl	3.7	1.8	5.7	10.0	1.6

SIRT3 – Relative decrease compared to Acetyl (acetyl/acyl)

	k_{cat}/K_m	k_5	k_{cat}	k_9	K_m
Acetyl	1.0	1.0	1.0	1.0	1.0
Hexanoyl	43.0	13.6	4.6	8.1	0.1
Decanoyl	3.5	9.5	2.8	6.5	0.8
Myristoyl	1.0	5.0	2.8	10.0	2.7

SIRT6 – Relative decrease to Myristoyl (myristoyl/acyl)

	k_{cat}/K_m	k_5	k_{cat}	k_9	K_m
Hexanoyl	22.2	31.8	4.4	18.3	0.2
Decanoyl	2.1	1.9	1.6	1.3	0.7
Myristoyl	1.0	1.0	1.0	1.0	1.0

SIRT1 - Relative decrease compared to Acetyl (acetyl/acyl)

	k_{cat}/K_m	k_{cat}	K_m
Acetyl	1.0	1.0	1.0
Hexanoyl	2.5	7.2	3.0
Decanoyl	1.3	14.4	9.7
Myristoyl	0.7	9.2	13.2